line width is much closer to the behavior expected for one-dimensional systems. In fact, it is known that the line shape is much more sensitive than the line width in recording deviations from ideal one-dimensional behavior, which can be determined either by interchain exchange, which effectively increases the magnetic dimensionality of the system, or by noncollinear dipolar interactions as in the present case.[29,36]

The line width in this case is difficult to express on first principles, because both the $(\gamma t)^{3/2}$ and ηt components must be taken into account. A simplified version was suggested by Mc Gregor et al.[37] according to which the peak-to-peak width ΔB_{pp} can be expressed as

$$\Delta B_{pp} = 1.09[M_2 + \rho M_{20}]/J \qquad (4)$$

where M_2 is the total second moment. If ρ is zero, the behavior is that of a normal exchange narrowed system, while if ρ is large the material goes closer to the one-dimensional limit.

Using this approach, the value of $\mathbf{D}_{jk}$ computed above, extending the sum only to nearest neighbors, and the coupling constant obtained from the fit of the magnetic susceptibility, we calculate the angular dependence of the line width as shown in Figure 4 with only ρ as an adjustable parameter. Given the simplification of the model the agreement with experiment can be considered as satisfactory. The very large value of $\rho = 70$, which is needed to fit the data, shows that the secular enhancement is indeed very large.

Conclusion

$Y(hfac)_3NITEt$ is a one-dimensional magnetic material in which the exchange interaction between the radicals is transmitted through a superexchange interaction with the metal orbitals. The EPR spectra show that indeed the material is highly one-dimensional even if marked deviations from ideal behavior are observed, essentially due to the zigzag nature of the chain.

Acknowledgment. Thanks are expressed to the Italian Ministry of Public Education and the CNR for financing the research. L.P. thanks Europa Metalli-LMI SpA for a research grant.

Supplementary Material Available: Table SI, containing experimental and crystallographic data, and Table SII, containing a complete listing of bond distances and angles (7 pages); Table SIII, listing observed and calculated structure factors (9 pages). Ordering information is given on any current masthead page.

---

(36) Hennessy, M. J.; McElwee, C. D. *Phys. Rev.* **1973**, *B7*, 930.
(37) McGregor, K. T.; Soos, Z. G. *J. Chem. Phys.* **1976**, *64*, 2506.

Contribution from the Laboratorium für chemische und mineralogische Kristallographie, Universität Bern, CH-3012 Bern, Switzerland, and Research School of Chemistry, The Australian National University, G.P.O. Box 4, Canberra, ACT 2601, Australia

Crystal and Molecular Structures of Encapsulated Ruthenium(II) and Ruthenium(III) Ions with Virtually Identical Geometries

Paul Bernhard,*,[1a,b] Hans-Beat Bürgi,*,[1a] Andrea Raselli,[1a] and Alan M. Sargeson*,[1c]

Received January 20, 1989

Single-crystal X-ray structure determinations at 130 K are reported for two encapsulated Ru compounds, $[Ru^{II}(Mesar)](CF_3SO_3)_2$ (II) and $[Ru^{III}(sar)](CF_3SO_3)_3$ (III) (Figure 1; sar = 3,6,10,13,16,19-hexaazabicyclo[6.6.6]eicosane; Mesar = 1-methyl derivative of sar). Compound II crystallizes in the orthorhombic space group *Pnma* with unit cell parameters $a = 21.941$ (4) Å, $b = 8.967$ (2) Å, $c = 13.078$ (2) Å (130 K), and $Z = 4$. For compound III the space group is $P\bar{3}c1$ (trigonal) with $a = b = 12.544$ (3) Å, $c = 22.638$ (5) Å, $\gamma = 120°$ (130 K), and $Z = 4$. The structure of II was refined to $R(F) = 0.038$ ($R_w(F) = 0.044$) for 2138 unique reflections with $F_o > 6\sigma(F_o)$. The structure of III was refined with use of a twin model to $R(F^2) = 0.073$ ($R_w(F^2) = 0.116$) for 2138 unique reflections with $F^2{}_o > 3\sigma(F^2{}_o)$. The two ions $Ru(Mesar)^{2+}$ and $Ru(sar)^{3+}$ exhibit virtually indistinguishable lel_3 geometries as illustrated by relevant structural parameters: $d(Ru\text{–}N)_{av} = 2.105$ (10) Å (II) and 2.097 (8) Å (III); $\alpha(Ru\text{–}en(bite))_{av} = 83.6$ (9)° (II) and 83.6 (2)° (III); trigonal twist = 49.7 (5)° (II) and 48.8 (2)° (III). By implication the activation free energy for structural reorganization of $Ru(sar)^{n+}$ (ΔG_{in}^*) in the electron-exchange reaction is negligible. Therefore, the rate constant ($k_{ex} = 1.2 \times 10^5$ M^{-1} s^{-1}, $T = 25$ °C, $\mu = 0.1$ M)[2] in this instance represents an upper limit imposed by the frequency factor, work term, and solvent reorganization. The value, in turn, can be used to calculate ΔG_{in}^* for other $M(sar)^{3+/2+}$ couples, i.e. $\Delta G_{in}^*(M) = RT \ln (k_{ex}(Ru)/k_{ex}(M))$. Results are (in kJ mol^{-1}) 22 (Mn), 5 (Fe), 38 (Co), and 10 (Ni), which correlate qualitatively with the structural differences between the M(II) and M(III) complexes. Possible relations between the structures and the low pK_a value for $Ru(sar)^{3+}$ (6.2–6.4)[3] and the regiospecific amine dehydrogenation in the cage cap are discussed.

Introduction

Electron-transfer reactions between Ru(II) and Ru(III) amine complexes are fast because only minor changes in coordination geometry occur upon oxidation or reduction of the metal. Where crystal structures are available for both oxidation states, Ru–N bond length changes are generally found to be ≤0.04 Å for aliphatic and ≤0.13 for aromatic amines (Table I). The fast self-exchange rate for the $Ru(sar)^{3+/2+}$ couple ($k_{ex} = 1.2 \times 10^5$ M^{-1} s^{-1}; sar = 3,6,10,13,16,19-hexaazabicyclo[6,6,6]eicosane, Figure 1)[2] was, therefore, not surprising and pointed to very similar structures of the ions. In order to obtain a quantitative measure of the similarity and differences between the two complexes with respect to bond lengths, angles, and ligand conformation, we carried out single-crystal X-ray structure determinations for the compounds $[Ru^{II}(Mesar)](CF_3SO_3)_2$ and $[Ru^{III}(sar)](CF_3SO_3)_3$ at low temperature (Mesar = 1-methyl derivative of sar). The methyl-substituted ligand was chosen because of serious disorder problems with several salts of the nonmethylated $Ru(sar)^{2+}$ cation. Further points of interest concern relationships between the structure of $Ru(sar)^{3+}$ and the acidity of the amine groups[3] as well as the selectivity of amine dehydrogenation, which is confined to the cage cap.[4]

---

(1) (a) Universität Bern. (b) Present address: Ciba-Geigy AG, CH-1701 Fribourg, Switzerland. (c) The Australian National University.
(2) Bernhard, P.; Sargeson, A. M. *Inorg. Chem.* **1987**, *26*, 4122.
(3) Bernhard, P.; Sargeson, A. M.; Anson, F. C. *Inorg. Chem.* **1988**, *27*, 2754.
(4) Bernhard, P.; Sargeson, A. M. *J. Chem. Soc., Chem. Commun.* **1985**, 1516; *J. Am. Chem. Soc.* **1989**, *111*, 597.
(5) Stynes, H. C.; Ibers, J. A. *Inorg. Chem.* **1971**, *10*, 2304.
(6) Trehoux, J.; Nowogrocki, G.; Thomas, D. *C.R. Séances Acad. Sci., Ser. C* **1972**, *274*, 1384.
(7) Smolenaers, P. J.; Beattie, J. K.; Hutchinson, N. D. *Inorg. Chem.* **1981**, *20*, 2202.
(8) Peresie, H. J.; Stanko, J. A. *J. Chem. Soc. D* **1970**, 1674.
(9) Gress, M. E.; Creutz, C.; Quicksall, C. O. *Inorg. Chem.* **1981**, *20*, 1522.
(10) Wishart, J. F.; Bino, A.; Taube, H. *Inorg. Chem.* **1986**, *25*, 3318.

0020-1669/89/1328-3234$01.50/0

Table I. Bond Lengths[a] of Various Ru(II/III) Hexaaza Redox Couples

		$\langle Ru^{II}-N\rangle$, Å	$\langle Ru^{III}-N\rangle$, Å
$Ru(NH_3)_6$[5,6]		2.143 (3)	2.104 (4)
		2.137 (6)	
$Ru(en)_3$[7,8]		2.132 (3)	2.11 (2)
Ru(sar)[b]		2.105 (10)	2.097 (8)
$Ru(NH_3)_5(pyz)$[9]	NH_3	2.15 (1)	2.11 (1)
	pyz[e]	2.006 (4)	2.076 (4)
$Ru(NH_3)_5$(*N*-Mepyz)[10]	NH_3	2.14 (2)	2.11 (1)
	N-Mepyz[e]	1.954 (4)	2.083 (4)
cis-$Ru(NH_3)(isn)_2$[11]	NH_3	2.15 (2)	2.12 (1)
	isn[e]	2.06 (1)	2.10 (1)
$[Ru(NH_3)_5]_2(pyz)$[12]	NH_3	2.14 (1)[c]	2.10 (1)[d]
	pyz[e]	2.013 (3)[c]	2.115 (1)[d]
$Ru(2,2'\text{-bpy})_3$[13,e]		2.055 (5)	
$Ru(py)_6$[14,e]		2.12 (2)	
$Ru(NCCH_3)_6$[15]		2.01 (1)	

[a] In $Ru(NH_3)_{6-x}L_x$ complexes Ru–NH_3 distances are averaged. [b] This work; for Ru(II), $Ru(Mesar)^{2+}$. [c] In $[Ru^{II}]_2$. [d] In $[Ru^{III}]_2$. [e] pyz = pyrazine; *N*-Mepyz = *N*-methylpyrazinium; isn = isonicotinamide; 2,2′-bpy = 2,2′-bipyridine; py = pyridine.

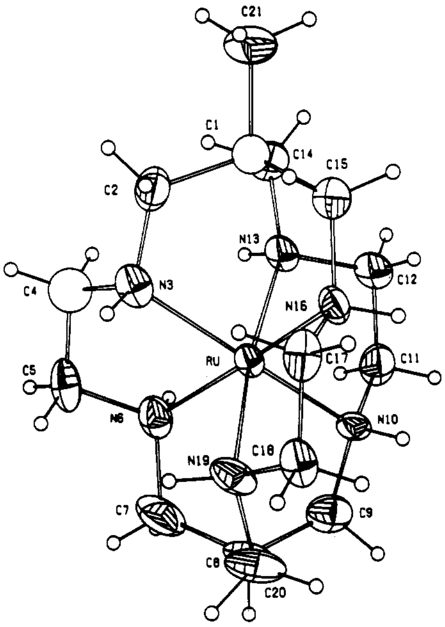

Figure 1. Atomic numbering in $Ru(1\text{-}Mesar)^{2+}$ (1-Mesar is 1-methyl-3,6,10,13,16,19-hexaazabicyclo[6.6.6]eicosane). $Ru(sar)^{3+}$ is identical except for an H atom replacing the CH_3 group.

Experimental Section

Syntheses and Crystal Growth. The compounds $[Ru(Mesar)](CF_3SO_3)_2$ (II) and $[Ru(sar)](CF_3SO_3)_3$ (III) were synthesized according to published procedures.[4] Light yellow crystals of II were grown by slow evaporation of a saturated aqueous solution with a gentle stream of argon over 2 days in the dark. Light yellow crystals of III were grown by slowly cooling a saturated solution of the compound in anhydrous acetonitrile to −20 °C. A large icosahedrally shaped crystal was then partially dissolved in acetonitrile until a sphere approximately 0.15 mm in diameter was obtained. Crystals were mounted on quartz needles. Densities were measured by flotation in dibromoethane/chlorobenzene at room temperature.

Data Collection. Data were collected on an Enraf-Nonius CAD4 diffractometer with graphite-monochromated MoKα radiation and a low-temperature attachment. Unit cell parameters for II and III were refined with use of 14 well-centered reflections in the θ range 12–15° at 273 K. The temperature was lowered in steps of ~40 K to 130 K, the cell parameters being refined after each step. A slight recentering of the crystals was necessary at the lowest temperature. During data collection the orientation was checked every 100 reflections and three reflections were used to monitor crystal decay. For II intensity losses were <0.2% and data were not corrected for decay. For III losses were up to 3% and data were corrected. For crystal data see Table II. Data collection parameters are given as supplementary material.

Table II. Crystallographic Data for $[Ru(Mesar)](CF_3SO_3)_2$ (II) and $[Ru(sar)](CF_3SO_3)_3$ (III)

	II	III
chem formula	$RuS_2F_6O_6N_6C_{17}H_{34}$	$RuS_3F_9O_9N_6C_{17}H_{32}$
a, Å	21.941 (4)	12.544 (3)
b, Å	8.967	12.544 (3)
c, Å	13.078 (2)	22.638 (5)
β, deg		120
V, Å^3	2573.0	3048.9
Z	4	4
fw	697.7	832.7
space group	*Pnma* (No. 62)	$P\bar{3}c1$ (No. 165)
T, K	130	130
λ, Å	0.71069	0.71069
ρ_{obs}, g cm^{-3}	1.75 (1)[a]	1.76 (1)[a]
ρ_{calc}, g cm^{-3}	1.801[b]	1.79 (3)[b]
μ, cm^{-1}	7.6	7.3
transmission coeff	0.91–0.89	0.86
$R(F_o)$	0.038	0.037[c]
$R_w(F_o)$	0.043	0.060[c]

[a] At 293 K. [b] At 130 K. [c] Using $R(F_o) = 1 - (1 - R(F_o^2))^{1/2}$.

Toward the end of the measurement the crystal of II cracked as indicated by broadened reflection profiles and visual inspection. An absorption correction could therefore not be done. A spherical absorption correction was done for III. Agreement factors obtained for multiple measurements and equivalent reflections are $R(F^2) = 0.014$ for II and $R(F^2) = 0.020$ for III.

Solution and Refinement of the Structures. (a) $[Ru^{II}(Mesar)](CF_3SO_3)_2$. Density measurement showed that the unit cell contained four complex cations (with approximate 32 symmetry). This implied either an ordered structure in space group $Pna2_1$ or a disordered structure in *Pnma*. Patterson and subsequent Fourier calculation in *Pnma* showed the 3-fold axis of the ligand to be slightly tilted with respect to the mirror plane, leading to a range of partial overlap between the atoms of the disordered complex cation. Non-hydrogen atoms were refined anisotropically (except for C1 and C4, which are close to the mirror plane and were refined isotropically). After inclusion of hydrogens as riding atoms with an isotropic displacement parameter the full-matrix least-squares refinement converged to $R = 0.04$ ($R_w = 0.045$). Nine atoms (Ru, S1, O11, C22, F11, O21, C23, F21, C5) had fixed y coordinates (0.25); i.e. they lie on the mirror plane. Inspection of the refined coordinates showed that Ru was distinctly (0.07 Å) off the 3-fold axis of the ligand in the b direction, resulting in three long and three short Ru–N bond lengths (2.05–2.16 Å). In the final refinement the Ru y coordinate was allowed to vary, with use of the restraint that the Ru–N distances should lie within 0.02 Å of each other. This procedure led to a significantly improved R factor ($R = 0.038$, $R_w = 0.043$) and a refined Ru position on the 3-fold axis of the ligand. The average Ru^{II}–N bond length changed by <0.003 Å. The range in Ru–N distances is 2.094–2.119 Å.

A refinement in space group $Pna2_1$ led to $R = 0.064$ ($R_w = 0.072$) with significantly more parameters than in *Pnma* (342 vs 284), to high parameter correlation, and to some chemically unreasonable bond lengths. Final atomic positions are given in Table III.

(b) $[Ru^{III}(sar)](CF_3SO_3)_3$. The Patterson map showed two different sets of ruthenium–nitrogen and ruthenium–carbon vectors, one with high and one with low intensity, indicating two orientations of the coordination octahedron with respect to the crystallographic 3-fold axis. A disordered structure was refined, with use of restraints for each type of bond. In the last steps of refinement all atoms were refined anisotropically. The least-squares procedure converged to $R(F) = 0.161$ ($R_w(F) = 0.184$). The remaining minimum and maximum difference electron densities were −2.3 and 3.3 e/Å^3, respectively. A variance analysis of different $F(hkl)$ groups showed that the variance of the reflections with $l = 2n + 1$ was about twice as much as the variance for $l = 2n$. It was therefore concluded that a disorder model ($F(hkl) = F(hkl$, site 1) + $F(hkl$, site 2)) was inadequate and that a twinned-crystal model might be more appropriate. A least-squares program allowing the refinement of the twin

---

(11) Richardson, D. E.; Walker, D. D.; Sutton, J. E.; Hodgson, K. O.; Taube, H. *Inorg. Chem.* **1979**, *18*, 2216.

(12) Fürholz, U.; Joss, S.; Bürgi, H. B.; Ludi, A. *Inorg. Chem.* **1985**, *24*, 943.

(13) Rillema, D. P.; Jones, D. S.; Levy, H. A. *J. Chem. Soc., Chem. Commun.* **1979**, 849.

(14) Templeton, J. L. *J. Am. Chem. Soc.* **1979**, *101*, 4906.

(15) Brown, M.; Fontaine, X. L. R.; Greenwood, N. N.; Kennedy, J. D.; Thornton-Pett, M. *J. Chem. Soc., Dalton Trans.* **1987**, 1169.

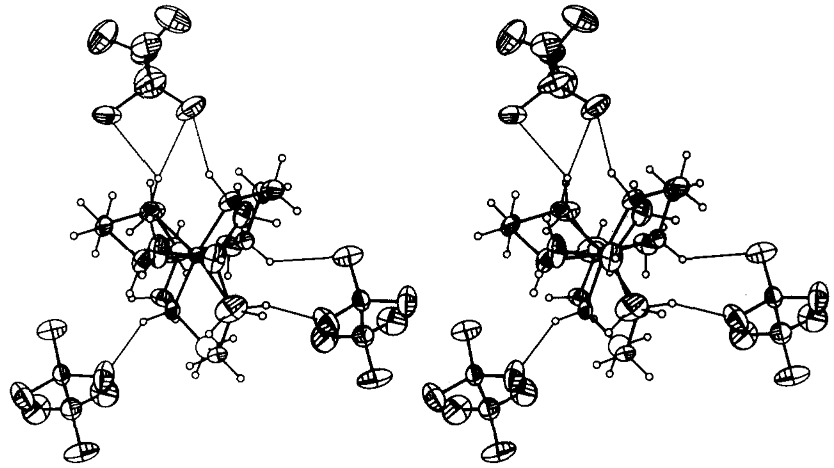

Figure 2. Stereoscopic view of $Ru(Mesar)^{2+}$ with surrounding $CF_3SO_3^-$ ions.

Table III. Final Atomic Positional Parameters and B_{eq} Values, with Standard Deviations in Parentheses, for $[Ru(Mesar)](CF_3SO_3)_2$

atom	x/a	y/b	z/c	B_{eq},[a] Å^2
Ru	0.34431 (2)	0.2410 (8)	0.31044 (4)	1.68 (3)
C1	0.4834 (3)	0.275 (1)	0.3249 (5)	2.7 (2)*
C2	0.4639 (4)	0.373 (1)	0.2321 (7)	3.1 (2)
N3	0.3991 (3)	0.3527 (7)	0.2027 (5)	2.4 (1)
C4	0.3895 (3)	0.271 (2)	0.1059 (6)	3.4 (2)*
C5	0.3234 (3)	$^1/_4$	0.0913 (5)	3.1 (1)
N6	0.2971 (3)	0.1710 (8)	0.1794 (5)	2.8 (1)
C7	0.2295 (4)	0.187 (1)	0.1877 (8)	4.6 (2)
C8	0.2077 (4)	0.205 (1)	0.2976 (8)	3.0 (2)
C9	0.2268 (8)	0.085 (2)	0.371 (1)	3.2 (3)
N10	0.2913 (3)	0.1051 (9)	0.4061 (5)	2.3 (1)
C11	0.3235 (7)	−0.045 (2)	0.410 (1)	3.1 (3)
C12	0.3917 (6)	−0.017 (2)	0.410 (1)	2.6 (2)
N13	0.4065 (3)	0.0639 (7)	0.3151 (5)	2.4 (1)
C14	0.4724 (4)	0.113 (1)	0.3114 (8)	3.5 (2)
C15	0.4585 (4)	0.338 (1)	0.4284 (7)	3.3 (2)
N16	0.3904 (3)	0.3496 (8)	0.4312 (5)	2.3 (1)
C17	0.3690 (6)	0.513 (2)	0.425 (1)	2.4 (3)
C18	0.3007 (6)	0.505 (1)	0.419 (1)	2.8 (3)
N19	0.2818 (3)	0.4193 (8)	0.3278 (6)	2.8 (1)
C20	0.2181 (7)	0.366 (2)	0.339 (1)	4.1 (4)
C21	0.5538 (4)	0.298 (2)	0.3314 (7)	5.1 (4)
S1	0.1311 (1)	$^1/_4$	0.6269 (1)	2.88 (3)
O11	0.1022 (3)	$^1/_4$	0.7266 (4)	4.9 (1)
O12	0.1624 (2)	0.3834 (4)	0.6034 (3)	4.76 (8)
C22	0.0662 (3)	$^1/_4$	0.5413 (5)	3.3 (1)
F11	0.0848 (2)	$^1/_4$	0.4442 (3)	5.2 (1)
F12	0.0315 (1)	0.3676 (4)	0.5543 (3)	5.49 (7)
S2	0.3340 (1)	0.261 (4)	0.6967 (2)	4.6 (2)
O21	0.2866 (2)	$^1/_4$	0.7698 (4)	4.3 (1)
O22	0.3425 (8)	0.417 (1)	0.6537 (8)	5.2 (3)
O23	0.3392 (8)	0.151 (1)	0.6230 (8)	5.5 (3)
C23	0.4038 (3)	$^1/_4$	0.7732 (5)	3.7 (1)
F21	0.4529 (2)	$^1/_4$	−0.7140 (4)	6.1 (1)
F22	0.4068 (1)	0.3680 (5)	0.8318 (3)	6.31 (8)

[a] Starred values denote atoms refined isotropically. Anisotropically refined atoms are given in the form of the isotropic equivalent thermal parameter.

Table IV. Final Atomic Positional Parameters and B_{eq} Values, with Standard Deviations in Parentheses, for $[Ru(sar)](CF_3SO_3)_3$

atom	x/a	y/b	z/c	B_{eq}, Å^2
Ru	0.3333	0.6667	0.1236 (1)	2.135 (7)
C1	0.3333	0.6667	−0.0127 (3)	3.9 (1)
C2	0.4636 (6)	0.7107 (6)	0.0048 (2)	4.9 (1)
N3	0.4910 (4)	0.7389 (4)	0.0707 (2)	3.26 (6)
C4	0.5609 (5)	0.8717 (5)	0.0837 (2)	3.57 (9)
C5	0.5685 (4)	0.8857 (5)	0.1508 (2)	3.10 (8)
N6	0.4431 (4)	0.8201 (4)	0.1772 (2)	3.21 (6)
C7	0.4442 (6)	0.7882 (5)	0.2408 (2)	4.5 (1)
C8	0.3333	0.6667	0.2591 (3)	4.1 (1)
S	0.6968 (1)	0.6186 (1)	0.1288 (1)	3.86 (2)
O1	0.7387 (5)	0.5325 (4)	0.1305 (2)	5.90 (9)
O2	0.6272 (5)	0.6189 (6)	0.1789 (2)	6.5 (1)
O3	0.6400 (5)	0.6211 (6)	0.0739 (2)	7.3 (1)
C	0.8361 (6)	0.7597 (6)	0.1350 (9)	10.2 (4)
F1	0.9072 (7)	0.7694 (8)	0.0848 (6)	17.0 (4)
F2	0.8969 (6)	0.7649 (8)	0.1839 (6)	15.8 (4)
F3	0.8158 (5)	0.8522 (4)	0.1366 (7)	20.5 (5)

fraction p was used for further refinement ($F^2(hkl) = p[F^2(hkl, \text{twin } 1)] + (1 - p)[F^2(khl, \text{twin } 2)]$). It led to $R(F^2) = 0.073$, $R_w(F^2) = 0.116$, corresponding to $R(F) \approx 0.037$, $R_w(F) \approx 0.06$. The refined value of p is 0.673 (3). Hydrogen atoms were included as riding atoms with an isotropic displacement parameter. The resulting C–N and C–F bond distances are chemically more reasonable. The displacement parameters along the z direction of the CF_3 unit are smaller compared to those for the F refinement but are still very large. Final atomic positions are given in Table IV.

Further Comments on Refinement. Both structures are somewhat affected by problems arising from disorder (II) or twinning (III). In the structure of II the atoms C11, C12 and C18, C17 are almost on a mirror plane and are therefore not very well resolved from the mirrored atoms C18′, C17′ and C11′, C12′. This led to an appreciable variation in bond lengths; viz., C4–C5 = 1.476 Å, C11–C12 = 1.519 Å, and C17–C18 = 1.501 Å. Introducing further restraints in the least-squares refinement did not lead to significant improvment of the R value. We thus present the structure as it converged using only a restraint on the Ru–N distances, as mentioned earlier. A refinement with no constraint on the Ru–N distances leads to the same atomic parameters except for $y(\mathrm{Ru}) = 0.239$ (1) and $U_{22}(\mathrm{Ru}) = 0.014$ (3) Å^2. The correlation coefficient between the two is 0.997. The difference from the constrained refinement is less than 2 σ. There is no significant change in R factors ($R(F) = 0.038$, $R_w(F) = 0.043$). The mean Ru–N distance is unchanged at 2.104 (10) Å; the range is slightly larger (2.082–2.140 Å) than for the refinement with constraint.

In compound III the CF_3 subunit shows very large atomic displacement parameters, especially in the c direction. A split-atom model with split carbon atoms ~0.5 Å apart and split fluorine atoms ~1.0 Å apart gave a better fit to the data but was either physically (nonpositive-definite displacement tensor) or chemically (bond distances) unreasonable and was not pursued. Data reduction for II and III and most of the solution/refinement of II were performed by using the structure determination package (SDP) of Enraf-Nonius[16] on a PDP 11/34 computer. The final stages of the refinement as well as the solution and preliminary refinements of III were carried out with the SHELX76[17] program on an IBM 3080/180 computer. Twin refinements were performed with the program of Waters and Ibers,[18] modified by Jameson.[19] Stereoscopic drawings were prepared with the ORTEP program of the XTAL[20] program package. Neutral atom scattering factors included anomalous dispersion

---

(16) *Structure Determination Package* (*Version 1983*) *User's Manual*; B. A. Frenz & Associates and Enraf-Nonius: College Station, TX, and Delft, Holland, 1983.

(17) Sheldrick, G. M. *Shelx76 User's Manual*; University of Cambridge: Cambridge, England, 1976.

(18) Waters, J. M.; Ibers, J. A. *Inorg. Chem.* **1977**, *16*, 3273–3277.

(19) Jameson, G. B. *Acta Crystallogr.* **1982**, *A38*, 817–820.

(20) Hall, S. R.; Stewart, J. M. "*Ortep*"; *XTAL2.4 User's Manual*; Universities of Western Australia and Maryland: Nedlands, Australia, and College Park, MD, 1988.

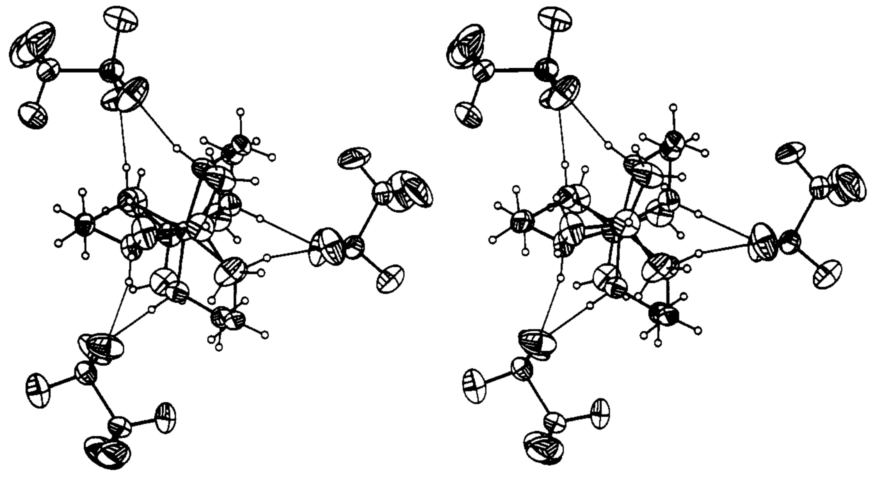

Figure 3. Stereoscopic view of $Ru(sar)^{3+}$ with surrounding $CF_3SO_3^-$ ions.

Table V. Selected Interatomic Distances (Å) and Angles (deg) for II and III

	II[a]	III[b]		II[a]	III[b]
			C1–C2	1.54 (4)	1.47 (1)
Ru–N3	2.104 (10)[c]	2.092 (6)	C2–N3	1.50 (1)	1.53 (1)
Ru–N6	2.105 (12)[c]	2.103 (6)	N3–C4	1.49 (4)	1.49 (1)
⟨Ru–N⟩	2.105 (10)	2.097 (8)	C4–C5	1.50 (2)	1.53 (1)
N3–Ru–N6	83.6 (9)	83.6 (2)	C5–N6	1.49 (3)	1.52 (1)
N3–Ru–N19	95.5 (1.1)	96.6 (3)	N6–C7	1.49 (1)	1.50 (1)
N3–Ru–N13	90.6 (3)	90.5 (2)	C7–C8	1.53 (3)	1.49 (1)
N6–Ru–N10	91.0 (1.3)	90.1 (2)	C1–C21	1.56 (1)	
Ru–N3–C2	114.8 (1.0)	113.8 (3)	C2–C1–C14	113.3 (1.2)	107.2 (4)
Ru–N3–C4	104.8 (7)	105.9 (4)	C2–C1–C21	105.3 (1.6)	
C2–N3–C4	113.0 (1.6)	113.2 (3)	C1–C2–N3	114.2 (1.5)	114.9 (5)
Ru–N6–C7	113.4 (9)	113.6 (3)	N3–C4–C5	107.1 (1.6)	113.2 (4)
Ru–N6–C5	106.9 (1.0)	107.6 (3)	C4–C5–N6	109.6 (1.6)	112.9 (4)
C5–N6–C7	111.5 (1.8)	112.7 (4)	N6–C7–C8	113.0 (1.0)	113.8 (4)
av	110.7	111.1	C7–C8–C9	114.0 (2.0)	110.4 (4)
conformation	C_3lel_3	C_3lel_3	N3–C4–C5–N6	−58.3 (1.7)	−54.8 (7)
N3, N6 twist	49.7 (5)	48.8 (5)	C4–C5–N6–C7	160.9 (1.2)	157.8 (5)
C2, C7 twist	46.0 (5)	45.1 (5)	C5–N6–C7–C8	−140.0 (1.1)	−145.2 (5)
ring puckering, *w*	47 (2)	44.7 (5)	⟨S-O⟩	1.43 (2)	1.43 (1)
C1–C8···C4–C5	4.3 (1.6)	5.7 (5)	⟨S-C⟩	1.82 (1)	1.765 (5)
C1–C2–N3–C4	−108.1 (1.2)	−105.9 (6)	⟨C-F⟩	1.32 (1)	1.35 (5)
C2–N3–C4–C5	174.8 (1.1)	173.7 (5)			

[a] Averaged with respect to C_3 axis (e.g. C1–C2, C1–C14, C1–C15); esd's of mean. [b] Complex has C_3 symmetry; esd's from structure factor least-squares calculation. [c] Bond lengths (Å): Ru–N3 = 2.106 (6); Ru–N6 = 2.098 (6); Ru–N10 = 2.099 (7); Ru–N13 = 2.094 (7); Ru–N16 = 2.113 (6); Ru–N19 = 2.119 (7).

corrections (f', f'') for all non-hydrogen atoms in the case of II and for the Ru, S, F, O, and N atoms in the case of III.[21]

Results and Discussion

Description of the Structures. The numbering used in the complexes is shown in Figure 1, and stereoscopic views of $Ru^{II}(Mesar)^{2+}$ and $Ru^{III}(sar)^{3+}$ with the surrounding counterions are shown in Figures 2 and 3, respectively.

In the structure of II one sulfonate (S1) group bridges two cations in the *b* direction, forming an infinite chain. The second counterion (S2) forms H-bonds to only one cation. One oxygen (O21) and one N–H group (N19–H19) do not engage in a H-bond. H···O distances range from 2.0 to 2.2 Å. In the structure of III, in which the complex lies on a 3-fold axis, each cation is surrounded by three H-bonding anions. There are two H-bonds per $-SO_3^-$ group of 1.9 and 2.0 Å. The H-bonds to $Ru^{III}(sar)^{3+}$ are thus more numerous and stronger than those to $Ru^{II}(Mesar)^{2+}$. This can be rationalized in terms of the higher acidity of the N–H protons in III.[3]

For the comparison of the two ions we have averaged distances and angles for II with respect to the molecular 3-fold axis. Table V shows that the geometries of the two complexes are virtually indistinguishable. All relevant parameters lie within 1 standard deviation! Variations are well within those expected from the different packing in the two lattices.

Compared to all reported structures of Ru(II) and Ru(III) hexaaza complexes (Table I), those of $Ru(Mesar)^{2+}$ and $Ru(sar)^{3+}$ have the most similar geometries. (It has been assumed that $Ru(bpy)_3^{2+}$ and $Ru(bpy)_3^{3+}$ should exhibit identical bond lengths because of the very fast self-exchange rate,[22] but this has yet to be substantiated by a crystal structure of $Ru(bpy)_3^{3+}$). Reasons for the generally small difference in Ru–N bond lengths between oxidation states II and III have been discussed.[23]

⟨Ru–N(aliphatic)⟩ values cluster around 2.14 Å for Ru(II) and around 2.10 Å for Ru(III) (Table I). The Ru^{II}–N distance is, therefore, surprisingly short in the cage complex. A possible explanation is based on the observation that in the M–N distance range 2.1–2.15 Å the trigonal twist angle of M(sar) and related complexes drops sharply from ~45 to ~30°.[24] It would seem that $Ru(Mesar)^{2+}$ has to choose between a structure with *d*-

---

[21] Cromer, D. T.; Waber, J. T. *International Tables for X-ray Crystallography*; Kynoch Press: Birmingham, England, 1974; Vol. IV, Tables 2.2, 2.3.1.

[22] Young, R. C.; Keene, F. R.; Meyer, T. J. *J. Am. Chem. Soc.* **1977**, *99*, 2468.

[23] Böttcher, W.; Brown, G. M.; Sutin, N. *Inorg. Chem.* **1979**, *18*, 1447.

[24] Comba, P.; Sargeson, A. M.; Engelhardt, L. M.; Harrowfield, J. M.; White, A. H.; Horn, E.; Snow, M. R. *Inorg. Chem.* **1985**, *24*, 2325.

(Ru–N) ≈ 2.15 Å and trigonal twist ~30° or one with *d*(Ru–N) ≈ 2.1 Å and trigonal twist ≥45°. The ligand field stabilization energy (LFSE) is more favorable for the latter since it is closer to the octahedron. The LFSE seems to dominate over the bond compression energy and to be largely responsible for the observed trigonal twist. A lower limit for the difference in ligand field stabilization may be estimated by using a force constant f_2 of ~2 mdyn $Å^{-1}$ for the Ru–N stretching vibration[32] and a Ru–N distance compression Δd of 0.035 Å: it follows that LFSE ≥ $6f_2(\Delta d)^2/2 \approx 4.4$ kJ mol^{-1}.

A comparison of the $Ru(en)_3$ fragment in $Ru(Mesar)^{2+}$ with the structure of $Ru(en)_3{}^{2+}$ itself[7] reveals three major differences. The respective values are 2.105 and 2.132 Å for *d*(Ru–N), 83.6 and 81.6° for the bite angle, and 49.7 and 52.9° for the trigonal twist angle. The differences may be understood from the following consideration: The N_3 triangle in $Ru(en)_3{}^{2+}$ to which the cap is to be attached has an edge length of ~3.1 Å; the N_3 triangle in a strain-free cap has an edge length of ~2.6 Å (with bond angles of 109.5° at the ternary carbon and 112° at the secondary carbon). In order to fit the two fragments together, both have to be distorted. In the $Ru(en)_3$ fragment the bite angle is increased by ~2° and the twist angle decreased by ~3°; in the cap the C–C–C angle is increased by ~4° and the C–C–N angle by ~2°. The resulting edge length of the N_3 triangle is ~3.0 Å. As a result of these distortions the N–C–C–N torsion angle in the five-membered chelate ring (puckering) decreases from 55.4 to 47°. In simple terms, the effect of the cap can be described as an apparent "pulling" in the direction of the 3-fold molecular axis.

Structure and Reactivity. The above arguments also help to interpret the extraordinarily low pK_a for $Ru(sar)^{3+}$ (6.2–6.4),[3] 6 orders of magnitude more acidic than $Ru(NH_3)_6{}^{3+}$ (pK_a = 12.4),[25] and the unusual stability of the deprotonated d^4 Ru(IV) complex.[3,4] Deprotonation leads to a substantial shortening of the Ru–N bond due to the strong π-interaction between the N lone pair of electrons and the partially empty t_{2g} orbitals on the metal; for a Ru^{IV}=N bond of this kind a length of 1.83 Å has been reported.[26] This shortening of the bond will reduce the average edge length of the N_3 triangle in the $Ru(en)_3$ fragment and thus lead to a reduction of angle strain in the cap.

A related question that has to be addressed in this context is the specificity of imine formation (or amine dehydrogenation) of $Ru(sar)^{3+}$, which is confined to the cap portion of the ligand.[4] From the structural point of view the angles Ru–N3–C2 and N3–C2–C1 seem to be better "prepared" than Ru–N3–C4 and N3–C4–C5 for the formation of an imine group in which the angles are expected to be close to 120°. The crucial parameters, however, are the pK_a's of the methylene groups and, in case the CH_2 deprotonation is not rate limiting, the rates of intramolecular electron transfer. The kinetic data did not allow a distinction between these possibilities, but a lower pK_a for C2 compared to that for C4 does not seem unreasonable in view of the strain in the C2 angle.

Finally we need to discuss the implication of the structural results for the electron self-exchange reaction

$$Ru(sar)^{3+} + {}^*Ru(sar)^{2+} \overset{k_{ex}}{\rightleftharpoons} Ru(sar)^{2+} + {}^*Ru(sar)^{3+} \quad (1)$$

and for those of other $M(sar)^{3+/2+}$ couples.[2] The activation energy for such processes is traditionally written as a sum of various contributions,[27] namely the Coulombic work term (w_r), the solvent reorganization energy ($\Delta G_{out}{}^‡$), and the inner-sphere activation energy ($\Delta G_{in}{}^‡$), arising from the structural differences between the oxidized and the reduced forms of the complex. Due to the similarity of the structures in the two oxidation states $\Delta G_{in}{}^‡$ for $Ru(sar)^{3+/2+}$ can be neglected. Assuming that the frequency factor, work term, and $\Delta G_{out}{}^‡$ (which depend only on the sizes and charges of the complexes) are constant for the various $M(sar)^{3+/2+}$ couples, $\Delta G_{in}{}^‡(M)$ may be calculated for M = Mn, Fe, Co, Ni:

$$\Delta G_{in}{}^‡(M) = RT \ln (k_{ex}(Ru)/k_{ex}(M)) \quad (2)$$

With $k_{ex}(M^{-1}\ s^{-1})$ [metal] = 17 [Mn], 6 × 10^3 [Fe], 2.1 [Co], and 1.7 × 10^3 [Ni],[2] the results are $\Delta G_{in}{}^‡$ (kJ mol^{-1}) = 22 [Mn], 5 [Fe],[28] 28 [Co], and 10 [Ni]. $\Delta G_{in}{}^‡(M)$ may be expressed in terms of the force constants f' [27] and the structural differences ξ_i between the two oxidation states as

$$\Delta G_{in}{}^‡ = (\textstyle\sum f_i'(\xi_{i,ox} - \xi_{i,red})^2/2)/2$$

$$f' = 2f_{ox}f_{red}/(f_{ox} + f_{red}) \quad (3)$$

If the ξ_i's are approximated by the six M–N bond distances, an effective force constant f' can be calculated that will also absorb contributions to $\Delta G_{in}{}^‡$ which are due to changes in ligand strain energy between ground and transition states. Using Δr values from crystallography (Mn, 0.11;[29] Fe, 0.04;[30] Co, 0.19;[24] Ni 0.09 Å[31]), we obtain f'(Mn) = 2 (1), f'(Fe) = 3 (7), f(Co) = 0.8 (0.2), and f'(Ni) = 1.5 (1.8) mdyn $Å^{-1}$. Uncertainties were estimated by assuming uncertainties in ln k_{ex} of 1.1 (factor of 3 in k_{ex}) and in Δr of 0.02 Å. The values of f' may be compared to those estimated from $\nu(A_{1g})$ for $M(NH_3)_6$ complexes[32] (Mn, 1.3;[33] Co, 1.7; Ni, 1.7 mdyn $Å^{-1}$ [33]). Two conclusions emerge: (1) The effective f' values are of the right order or magnitude, indicating that the inner-sphere contributions to $\Delta G^‡$ obtained from eq 2 are reasonable. (2) The effective f' value for $Co(sar)^{2+/3+}$ is significantly smaller than expected on the basis of bond distances alone (0.8 vs 1.7 mdyn $Å^{-1}$). This may be interpreted in terms of a decrease of ligand strain between ground- and transition-state structures of the $Co(sar)^{2+/3+}$ species. From the present result the individual contributions of the two complexes to the total strain release in the transition state (~28 kJ mol^{-1}) cannot be determined separately. These results from kinetic and diffraction experiments are in fair agreement with molecular mechanics calculations.[34] For 1,8-diamino-sar $\Delta G_{in}{}^‡$ was calculated to be between 45 (*lel*$_3$ conformation) and 32 kJ mol^{-1} (*ob*$_3$ conformation). The energy contribution due to Co–N reorganization alone is ~65 kJ mol^{-1} at $d(Co–N)^‡ \approx 2.05$ Å, leading to an estimated strain release of 20–33 kJ mol^{-1}. The calculation also shows that the strain energy of the cage is minimal at *d*(Co–N) ≈ 2.05 Å, indicating that the strain release in the transition state for electron transfer is due to contribution from both the $Co(sar)^{3+}$ and $Co(sar)^{2+}$ ions. Unfortunately the uncertainties in f' for Mn, Fe, and Ni are large and conclusions about the effects of ligand strain cannot easily be drawn for these metal ions. However, the present interpretation of structural and kinetic data so far represents the only attempt to quantify from experiment the influence of strain on electron-transfer reactivity.

Conclusion

Crystal structure determinations on two encapsulated Ru complexes, $Ru(Mesar)^{2+}$ and $Ru(sar)^{3+}$, reveal virtually identical geometries of the two ions with Ru–N bond lengths of 2.105 (10) Å (II) and 2.097 (8) Å (III). By implication the electron self-exchange rate constant of 1.2 × 10^5 M^{-1} s^{-1} represents an upper limit associated with the solvation and the charges of the cage

---

(25) Waysbort, D.; Navon, G. *J. Chem. Soc. D* **1971**, 1410.
(26) Adcock, P. A.; Keene, F. R.; Smythe, R. S.; Snow, M. R. *Inorg. Chem.* **1984**, *23*, 2336.
(27) Sutin, N. *Prog. Inorg. Chem.* **1983**, *30*, 441.
(28) This value is corrected for *K*(high spin/low spin) ≈ $2[k_{ex}(Fe, ls)] = [k_{ex}(Fe)](1 + K)$.
(29) Mn^{II}(sar): Reference 24. Mn^{III}(sar): Dean, C.; Snow, M. R.; Tiekink, E. R. T. Submitted for publication.
(30) From $Fe^{II}(tacn)_2$ and $Fe^{III}(tacn)_2$: Boeyens, J. C. A.; Forbes, A. G. S.; Hancock, R. D.; Wieghardt, K. *Inorg. Chem.* **1985**, *24*, 2926.
(31) Ni^{II}(sar): Reference 24. $Ni^{II}(tacn)_2$: Zompa, L. J.; Margulis, T. N. *Inorg. Chim. Acta* **1978**, *28*, L157. $Ni^{III}(tacn)_2$: Wieghardt, K.; Walz, W.; Nuber, B.; Weiss, J.; Ozarowski, A.; Stratemeier, H.; Reinen, D. *Inorg. Chem.* **1986**, *25*, 1650.
(32) Schmidt, K. H.; Müller, A. *Inorg. Chem.* **1975**, *14*, 2183.
(33) Estimates as in Reference 32 of: Bernhard, P.; Sargeson, A. M. *Inorg. Chem.* **1988**, *27*, 2582.
(34) Geue, R. J. Unpublished results.

complexes. There seems to be angular strain in the cage caps, whereas the en fragments exhibit angles close to the tetrahedral value. This is consistent with the ease of deprotonation and the observed specificity of amine dehydrogenation in Ru(sar)$^{3+}$.

Acknowledgment. P.B. thanks Prof. A. Ludi (Bern, Switzerland) for financial support. We gratefully acknowledge financial help by the "Schweizerischer Nationalfonds zur Förderung der wissenschaftlichen Forschung". We thank Prof. G. B. Jameson for a copy of his twin refinement program.[19]

Supplementary Material Available: Listings of calculated hydrogen positional parameters, anisotropic displacement parameters, crystal data, intensity collection, and refinement parameters, and hydrogen bond distances and angles (7 pages); listings of observed and calculated structure factors (18 pages). Ordering information is given on any current masthead page.

Contribution from the Departments of Chemistry, The University of Trondheim,
N-7055 Dragvoll, Trondheim, Norway, and The University of Reading, Whiteknights, Reading RG6 2AD, U.K.

Gas-Phase Electron Diffraction Study of Bis(dimethyldithiocarbamato)copper(II), [Cu(S_2CNMe$_2$)$_2$], and Bis(dimethyldithiocarbamato)zinc(II), [Zn(S_2CNMe$_2$)$_2$]

Kolbjørn Hagen,[1a] Catherine J. Holwill,[1b] and David A. Rice*,[1b]

Received January 31, 1989

The molecular structures of [Cu(S_2CNMe$_2$)$_2$] and [Zn(S_2CNMe$_2$)$_2$] have been studied by gas-phase electron diffraction. Both compounds are monomeric in the gas phase with the metal atoms being bound to two chelating [S_2CNMe$_2$] groups (r_g(Cu–S) = 2.284 (9) Å; r_g(Zn–S) = 2.348 (8) Å). The major difference between the two structures is in the geometry of the MS$_4$ fragments, that of the copper compounds being pseudo square planar (D_{2h}) while that of the zinc compound is pseudotetrahedral (D_{2d}). The reason for the difference is attributed to the availability in the copper(II) compound of crystal field stabilization energy that is greater than the repulsive energy of the steric interactions imposed by the metal adopting a coordination sphere of D_{2h} symmetry. Selected bond lengths and angles in the [S_2CNMe$_2$] groups are as follows (the data for the copper compound are quoted first with those for the zinc species being in brackets): r_g(C—S) = 1.716 (10) Å [1.727 (10) Å]; r_g(C=N) = 1.334 (18) Å [1.351 (17) Å]; r_g(C—N) = 1.476 (18) Å [1.479 (17) Å]; $\angle_\alpha$S—M—S(chelate angle) = 78.78 (69)° [79.68 (59)°]; $\angle_\alpha$C=N—C = 124.9 (1.3)° [122.5 (1.2)°].

Introduction

The geometry of the coordination sphere exhibited by a metal in one of its complexes can often be predicted from a consideration of simple crystal field theory, a knowledge of the d^n configuration of the metal, and the nature of the ligands in the compound. For example nickel(II), which is d^8, is expected to form square-planar complexes with ligands high in the spectrochemical series and tetrahedral ones with ligands low in the series. Thus, [NiCl$_4$]$^{2-}$ was predicted to be tetrahedral and [Ni(CN)$_4$]$^{2-}$ square planar. Confirmation of the predictions was achieved through single-crystal X-ray diffraction studies. However, in the solid state, packing forces may influence the coordination geometry exhibited by a metal ion; thus, the agreement between prediction and the results of single-crystal X-ray diffraction studies may be fortuitous. In the gas phase packing forces are eliminated; thus, the comparison between prediction and the structural results from gas-phase electron diffraction studies provide a valid test for predictions. However, while there have been numerous studies of coordination compounds by single-crystal X-ray diffraction, only a small number have been examined by gas-phase electron diffraction and those that have been studied possess either oxygen or nitrogen in the coordination sphere. Crystal effects are important. For example, with the ligand [MeCOCHCOMe]$^-$, which is low in the spectrochemical series, nickel(II) forms [Ni(MeCOCHCOMe)$_2$], which is trimeric in the solid state with all three metal atoms being six-coordinate,[2] while in the gas phase it is monomeric with the metal having a planar (pseudo square planar) coordination sphere of four oxygen atoms.[3]

In view of the paucity of electron diffraction data for coordination compounds and yet the usefulness of such data that do exist, we decided to attempt to extend the range of compounds that have been studied in the gas phase to some simple compounds having sulfur ligands. We now report a study of the structures of bis(dimethyldithiocarbamato)copper(II), [Cu(S_2CNMe$_2$)$_2$], and bis(dimethyldithiocarbamato)zinc(II), [Zn(S_2CNMe$_2$)$_2$]. The existence of reports of single-crystal X-ray studies on both compounds[4,5] influenced the choice of compounds for investigation.

Experimental Section and Analysis of the Structure

Preparation of Bis(dimethyldithiocarbamato)zinc(II), [Zn(S_2CNMe$_2$)$_2$], and Bis(dimethyldithiocarbamato)copper(II), [Cu(S_2CNMe$_2$)$_2$]. Zinc(II) chloride or copper(II) chloride (0.01 mol) was dissolved in the minimum quantity of ethanol. To this was added a saturated ethanolic solution of sodium dimethyldithiocarbamate (0.02 mol). Immediate precipitation took place, and the compounds were isolated by filtration and washed with ethanol. The samples had metal, carbon, hydrogen, and nitrogen analyses in accord with the formulation [M(S_2CNMe$_2$)$_2$] (M = Cu, Zn).

The Reading Apparatus. Electron diffraction data were obtained by using the apparatus built at the Univeristy of Reading. Full details of the apparatus have been given elsewhere.[6]

The experimental conditions used to obtain data for [Zn(S_2CNMe$_2$)$_2$] and [Cu(S_2CMe$_2$]] are as follows. Three plates were examined at both long and short camera distances for both compounds, the camera distances being 494.51 and 244.33 mm. The electron wavelength was 0.061 54 Å. The nozzle temperatures were 275 °C for the copper species and 260 °C for the zinc compound. Unfortunately the s range of the usable data was restricted to 3.75–12.00 and 9.00–25.00 Å^{-1} for the long and short camera distances, respectively. This cutoff for usuable data, 12.00 and 25.00 Å^{-1} for the long and short camera distances, respectively, we believe is caused by sample being deposited upon the plate when high nozzle temperatures are used. This effect has been noted previously.[6]

The experimental data were processed as previously described[7–11] with

---

* To whom correspondence should be addressed.

(1) (a) The University of Trondheim. (b) The University of Reading.
(2) Bullen, J. C.; Mason, R.; Pauling, P. *Inorg. Chem.* **1965**, *4*, 456.
(3) Shibata, S.; Ohia, M.; Tani, R. *J. Mol. Struct.* **1981**, *73*, 119.
(4) Einstein, F. W. B.; Field, J. S. *Acta Crystallogr.* **1974**, *B30*, 2928.
(5) Klug, H. P. *Acta Crystallogr.* **1966**, *21*, 536.
(6) Holwill, C. J. Ph.D. Thesis, University of Reading, Reading, U.K., 1987.
(7) Hagen, K.; Hedberg, K. *J. Am. Chem. Soc.* **1973**, *95*, 1003.
(8) Gundersen, G.; Hedberg, K. *J. Chem. Phys.* **1969**, *51*, 2500.
(9) Andersen, B.; Seip, H. M.; Strand, T. G.; Stølevik, R. *Acta Chem. Scand.* **1969**, *23*, 3224.
(10) Hagen, K.; Hobson, R. J.; Holwill, C. J.; Rice, D. A. *Inorg. Chem.* **1986**, *25*, 3659.
(11) Hedberg, L. *Abstracts of Papers*, 5th Austin Symposium on Gas-Phase Molecular Structure, Austin, TX, March 1974; p 37.

0020-1669/89/1328-3239$01.50/0